
One-Shot Domain Decomposition Methods for Shape Optimization Problems

Rongliang Chen¹ and Xiao-Chuan Cai²

¹ College of Mathematics and Econometrics, Hunan University, Changsha, Hunan 410082, China (rlchen@hnu.edu.cn)

² Department of Computer Science, University of Colorado at Boulder, Boulder, CO 80309, USA (cai@cs.colorado.edu)

1 Introduction

Shape optimization aims to optimize an objective function by changing the shape of the computational domain. In recent years, shape optimization has received considerable attentions. On the theoretical side there are several publications dealing with the existence of solution and the sensitivity analysis of the problem; see e.g., [6] and references therein. On the practical side, optimal shape design has played an important role in many industrial applications, for example, aerodynamic shape design [7], artery bypass design [1, 10], and so on. In this paper, we propose a general framework for the parallel solution of shape optimization problems, and study it in detail for the optimization of an artery bypass problem.

For PDE constrained optimization problems, there are two basic approaches: *nested analysis and design* and *simultaneous analysis and design* (one-shot methods). As computers become more powerful in processing speed and memory capacity, one-shot methods become more attractive due to their higher degree of parallelism, better scalability, and robustness in convergence. The main challenges in the one-shot approaches are that the nonlinear system is two to three times larger, and the corresponding indefinite Jacobian system is a lot more ill-conditioned and also much larger. So design a preconditioner that can substantially reduce the condition number of the large fully coupled system and, at the same time, provides the scalability for parallel computing becomes a very important stage in the one-shot methods. There are several recent publications on one-shot methods for PDE constrained optimization problems. In [5], a reduced Hessian sequential quadratic programming method was introduced for an aerodynamic design problem. In [4], a parallel *full space method* was introduced for the boundary control problem where a Newton-Krylov method is used together with Schur complement type preconditioners. In [9] and [8], an overlapping Schwarz based Lagrange-Newton-Krylov approach (LNKSz) was investigated for some boundary control problems. As far as we know no one has studied shape optimization problems using LNKSz, which has the potential to solve very large problems on machines with a large number of processors (np). The previ-

ous work on LNKSz doesn't consider the change of the computational domain which makes the study much more difficult and interesting.

2 Shape Optimization on a Moving Mesh

We consider a class of shape optimization problems governed by the stationary incompressible Navier-Stokes equations defined in a two dimensional domain Ω_α . Our goal is to computationally find the optimal shape for part of the boundary $\partial\Omega_\alpha$ such that a given objective function J_o is optimized. We represent the part of the boundary by a smooth function $\alpha(x)$ determined by a set of parameters $\mathbf{a} = (a_1, a_2, \dots, a_p)$. By changing the shape defined by $\alpha(x)$, one can optimize certain properties of the flow. In this paper, we focus on the minimization of the energy dissipation in the whole flow field and use the integral of the squared energy deformation as the objective function [6]

$$\begin{aligned} \min_{\mathbf{u}, \alpha} J_o(\mathbf{u}, \alpha) &= 2\mu \int_{\Omega_\alpha} \boldsymbol{\varepsilon}(\mathbf{u}) : \boldsymbol{\varepsilon}(\mathbf{u}) dx dy + \frac{\beta}{2} \int_I (\alpha'')^2 dx \\ \text{subject to} & \\ \left\{ \begin{array}{ll} -\mu \Delta \mathbf{u} + \mathbf{u} \cdot \nabla \mathbf{u} + \nabla p = \mathbf{f} & \text{in } \Omega_\alpha, \\ \nabla \cdot \mathbf{u} = 0 & \text{in } \Omega_\alpha, \\ \mathbf{u} = \mathbf{g} & \text{on } \Gamma_{inlet}, \\ \mathbf{u} = \mathbf{0} & \text{on } \Gamma_{wall}, \\ \mu \frac{\partial \mathbf{u}}{\partial \mathbf{n}} - p \cdot \mathbf{n} = \mathbf{0} & \text{on } \Gamma_{outlet}, \\ \alpha(a) = z_1, \quad \alpha(b) = z_2, & \end{array} \right. \end{aligned} \tag{1}$$

where $\mathbf{u} = (u, v)$ and p represent the velocity and pressure, \mathbf{n} is the outward unit normal vector on $\partial\Omega_\alpha$ and μ is the kinematic viscosity. Γ_{inlet} , Γ_{outlet} and Γ_{wall} represent the inlet, outlet and wall boundaries, respectively; see Fig. 1. \mathbf{f} is the given body force and \mathbf{g} is the given velocity at the inlet Γ_{inlet} . $\boldsymbol{\varepsilon}(\mathbf{u}) = \frac{1}{2}(\nabla \mathbf{u} + (\nabla \mathbf{u})^T)$ is the deformation tensor for the flow velocity \mathbf{u} and β is a nonnegative constant. $I = [a, b]$ is an interval in which the shape function $\alpha(x)$ is defined. In the constraints, the first five equations are the Navier-Stokes equations and boundary conditions and the last two equations indicate that the optimized boundary should be connected to the rest of the boundary and z_1 and z_2 are two given constants. The last term in the objective function is a regularization term providing the regularity of $\partial\Omega_\alpha$.

The optimization problem (1) is discretized with a LBB-stable (*Ladyzhenskaya-Babuška-Brezzi*) $Q_2 - Q_1$ finite element method. Since the computational domain of the problem changes during the optimization process, the mesh needs to be modified following the computational domain. Generally speaking, there are two strategies to modify the mesh. One is mesh reconstruction which often guarantees a good new mesh but is computationally expensive. The other strategy is moving mesh which is cheaper but the deformed mesh may become ill-conditioned when the boundary variation is large. In our test case the boundary variations are not very large, so we

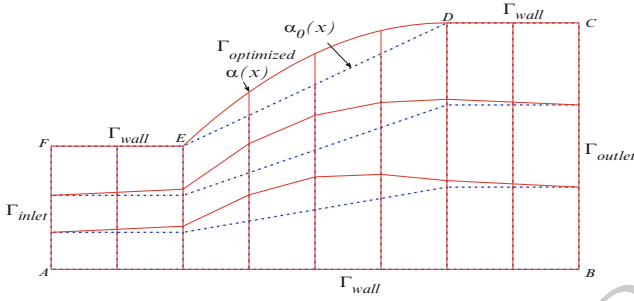


Fig. 1. The initial domain Ω_{α_0} (dashed line) and deformed domain Ω_{α} (solid line) over a simple mesh. The boundary $\Gamma_{optimized}$ (ED) denotes the part of the boundary whose shape is computed by the optimization process

use the latter strategy. The moving of the mesh is simply described by Laplace's equations. 68
69

$$\begin{cases} -\Delta \delta_{\mathbf{x}} = \mathbf{0} & \text{in } \Omega_{\alpha_0}, \\ \delta_{\mathbf{x}} = \mathbf{g}_{\alpha} & \text{on } \partial\Omega_{\alpha_0}, \end{cases} \quad (2)$$

where $\delta_{\mathbf{x}}$ is the mesh displacement and $\mathbf{g}_{\alpha} = (g_{\alpha}^x, g_{\alpha}^y)$ is the displacement on the boundary determined by $\alpha(x)$. Note that \mathbf{g}_{α} is obtained automatically during the iterative solution process. For example, in Fig. 1, $g_{\alpha}^x = 0$ and $g_{\alpha}^y = \alpha(x) - \alpha_0(x)$. The Eqs. (2) are discretized with a Q_2 finite element method. The discretized shape optimization problem is given as follows 70
71
72
73
74

$$\begin{aligned} \min_{\mathbf{u}, \mathbf{a}, \delta_{\mathbf{x}}} J_o(\mathbf{u}, \mathbf{a}, \delta_{\mathbf{x}}) &= \mu \mathbf{u}^T \mathbf{J} \mathbf{u} + \frac{\beta}{2} \mathbf{J}_{\alpha} \\ \text{subject to} & \\ \begin{cases} \mathbf{K} \mathbf{u} + \mathbf{B}(\mathbf{u}) \mathbf{u} - \mathbf{Q} \mathbf{p} &= \mathbf{F}_f + \mathbf{F}_u, \\ \mathbf{Q}^T \mathbf{u} &= \mathbf{0}, \\ \mathbf{D} \delta_{\mathbf{x}} &= \mathbf{F}_x, \\ \mathbf{A}_a &= \mathbf{F}_a. \end{cases} \end{aligned} \quad (3)$$

Here \mathbf{F}_f refers to the discretized body force, \mathbf{F}_u and \mathbf{F}_x refer to the Dirichlet boundary condition for \mathbf{u} and $\delta_{\mathbf{x}}$, respectively, and \mathbf{A}_a and \mathbf{F}_a are the geometric constrains. Note that \mathbf{K} , $\mathbf{B}(\mathbf{u})$, \mathbf{Q} and \mathbf{J} depend on the grid displacement $\delta_{\mathbf{x}}$, while \mathbf{D} is independent of $\delta_{\mathbf{x}}$. Here $\delta_{\mathbf{x}}$ is treated as an optimization variable and the moving mesh equations are viewed as constraints of the optimization problem which are solved simultaneously with the other equations. 75
76
77
78
79
80

3 One-Shot Lagrange-Newton-Krylov-Schwarz Methods 81

We use a Lagrange multiplier method to transform the optimization problem (3) to a nonlinear system $\mathbf{G}(\mathbf{X}) = \mathbf{0}$ which is solved by an inexact Newton method. 82
83

Given an initial guess \mathbf{X}^0 , at each iteration, $k = 0, 1, \dots$, we use a GMRES method to approximately solve the preconditioned system

$$\mathbf{H}^k(\mathbf{M}^k)^{-1}(\mathbf{M}^k \mathbf{d}^k) = -\mathbf{G}^k, \tag{4}$$

to find a search direction \mathbf{d}^k , where $\mathbf{H}^k = \nabla_{\mathbf{X}} \mathbf{G}(\mathbf{X}^k)$ is the Jacobian matrix of the nonlinear function, $\mathbf{G}^k = \mathbf{G}(\mathbf{X}^k)$ and $(\mathbf{M}^k)^{-1}$ is an additive Schwarz preconditioner [11] defined as

$$(\mathbf{M}^k)^{-1} = \sum_{l=1}^{N_p} (R_l^\delta)^\mathbf{T} (\mathbf{H}_l^k)^{-1} R_l^\delta,$$

where $\mathbf{H}_l^k = R_l^\delta \mathbf{H}^k (R_l^\delta)^\mathbf{T}$, R_l^δ is a restriction operator from Ω_α to the overlapping subdomain, δ is the size of the overlap which is understood in terms of the number of elements; i.e., $\delta = 8$ means the overlapping size is 8 layers of elements, and N_p is the number of subdomains which is equal to np in this paper. After approximately solving (4), the new approximate solution is defined as $\mathbf{X}^{k+1} = \mathbf{X}^k + \tau^k \mathbf{d}^k$, and the step length τ^k is selected by a cubic line search.

4 Numerical Experiments

The algorithm introduced in the previous sections is applicable to general shape optimization problems governed by incompressible Navier-Stokes equations. Here we study an application of the algorithm for the incoming part of a simplified artery bypass problem¹ [2] as shown in Fig. 2. Our solver is implemented using PETSc [3]. All computations are performed on an IBM BlueGene/L supercomputer at the National Center for Atmospheric Research. Unstructured meshes, which are generated with CUBIT and partitioned with ParMETIS, are used in this paper.

this figure will be printed in b/w

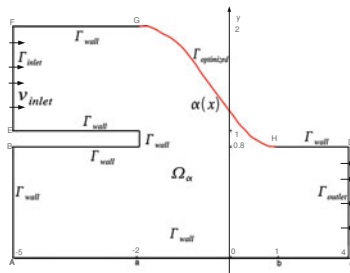


Fig. 2. The incoming part of a simplified bypass model; The red boundary $\Gamma_{optimized}$ denotes the part of the boundary whose shape is to be determined by the optimization process

¹ This is the incoming part of a bypass: [www.reshealth.org/images/greystone/em\delimiter"026E30F_2405.gif](http://www.reshealth.org/images/greystone/em\delimiter)

Without the blockage, the flow is supposed to go from AB to CD, but now we assume that AB is blocked and the flow has to go through EF. For simplicity, we let the thickness EF be fixed and the body force $\mathbf{f} = \mathbf{0}$ in the Navier-Stokes equations. The shape of the bypass is determined by the curve GH as in Fig. 2. The boundary conditions on the inlet Γ_{inlet} are chosen as a constant v_{in} , no-slip boundary conditions are used on the walls Γ_{wall} . On the outlet section Γ_{outlet} , the free-stress boundary conditions are imposed; see (1). We use a polynomial $\alpha(x) = \sum_{i=1}^p a_i x^i$ with $p = 7$ to represent the part of the boundary that needs to be optimized. Other shape functions can be used, but here we simply follow [1]. The goal is to compute the coefficients $\mathbf{a} = (a_1, \dots, a_p)$, such that the energy loss is minimized.

In all experiments, we use a hand-coded Jacobian matrix. The Jacobian system in each Newton step is solved by a right-preconditioned restarted GMRES with an absolute tolerance of 10^{-10} , a relative tolerance of 10^{-3} , and a restart at 100. We stop the Newton iteration when the nonlinear residual is decreased by a factor of 10^{-6} .

this figure will be printed in b/w

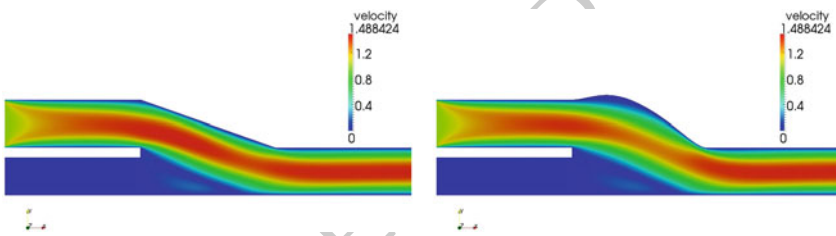


Fig. 3. Velocity distribution of the initial (left) and optimal shapes (right). The initial shape is given by a straight line. $\beta = 0.01$ and $Re = 100$

this figure will be printed in b/w

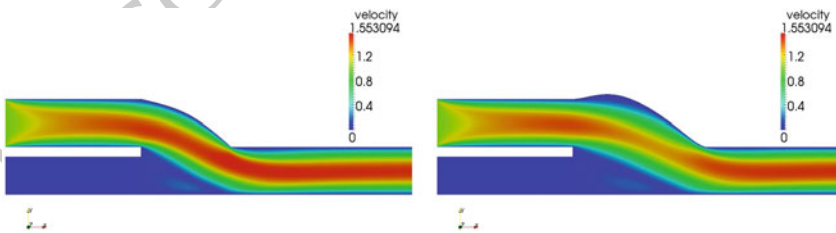


Fig. 4. Velocity distribution of the initial (left) and optimal shapes (right). The initial shape is given as $\alpha(x) = 0.4 + 0.45x^2 + 0.15x^3$. $\beta = 0.01$ and $Re = 100$

In the first test case, we set the Reynolds number $Re = \frac{Lv_{in}}{\mu}$ to 100, where $L = 1.0$ cm is the artery diameter, $v_{in} = 1.0$ cm/s is the inlet velocity and $\mu = 0.01$ cm²/s.

We solve the problem on a mesh with about 18,000 elements. $\beta = 0.01$ and the degrees of freedom (DOF) is 589,652. The initial shape is given by a straight line, and Fig. 3 shows the velocity distribution of the initial (left) and optimal shapes (right). The energy dissipation of the optimized shape is reduced by about 5.13 % compared to the initial shape. Figure 4 is the velocity distribution of another initial shape (left) which is given as $\alpha(x) = 0.4 + 0.45x^2 + 0.15x^3$ and the corresponding optimal shape (right). The reduction of the energy dissipation of this case is about 11.96 %. Figures 3 and 4 show that we can obtain nearly the same optimal shape from different initial shapes.

In the test case showed in Fig. 3, if we add a small inlet velocity at the boundary AB, which is equal to that the blood flow is not totally blocked, the computed optimal shape would be different from what is shown in Fig. 3. If we move the boundary AB towards CD (A from $(-5, 0)$ to $(-3, 0)$ and B from $(-5, 0.8)$ to $(-3, 0.8)$), the optimal shape is nearly the same as Fig. 3 since the flow in the “dead area” doesn’t impact much of the optimal solution.

this figure will be printed in b/w

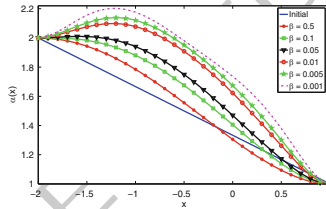


Fig. 5. The initial shape and optimal shapes with different values of parameter β . $DOF = 589,652$ and $Re = 100$

The regularization parameter β in the objective function is very important for shape optimization problems. From Table 1 we see that reducing β can increase the reduction of the energy dissipation (“Init.”, “Opt.” and “Reduction” are the initial, optimized and reduction of the energy dissipation in the table), but the number of Newton (Newton) and the average number of GMRES iterations per Newton (GMRES) and the total compute time in seconds (Time) increase, which means that the nonlinear algebraic system is harder to solve when β is small. This is because the boundary of Ω_α is more flexible and may become irregular when β is too small. Figure 5 shows the initial shape and the optimized shapes obtained with different values of β . From this figure we see that β controls the boundary deformation.

To show the parallel scalability of the algorithm, two meshes with $DOF = 589,652$ and $DOF = 928,572$ are considered. The strong scalability of our algorithm is good; see Fig. 6 and Table 2, which show that the speedup is almost linear when np is small. As expected in one-level Schwarz methods, the preconditioner becomes worse as the number of subdomains increases.

Table 3 shows some results for different Re . Judging from the increase of the number of linear and nonlinear iterations, it is clear that the problem becomes harder

Table 1. Effect of the parameter β . $DOF = 589,652$, $Re = 100$.

| β | Newton | GMRES | Time | Energy Dissipation | | |
|---------|--------|--------|--------|--------------------|------|-----------|
| | | | | Init. | Opt. | Reduction |
| 0.05 | 4 | 386.00 | 477.89 | 1.17 | 1.12 | 4.27% |
| 0.01 | 5 | 441.40 | 600.86 | 1.17 | 1.11 | 5.13% |
| 0.005 | 5 | 439.00 | 599.77 | 1.17 | 1.10 | 5.98% |
| 0.001 | 6 | 510.67 | 747.78 | 1.17 | 1.10 | 5.98% |

Table 2. Parallel scalability for two different size grids. $\beta = 0.1$, $overlap = 6$ and $Re = 100$.

| np | $DOF = 589,652$ | | | $DOF = 928,572$ | | |
|------|-----------------|--------|---------|-----------------|--------|---------|
| | Newton | GMRES | Time | Newton | GMRES | Time |
| 32 | 4 | 124.50 | 2959.73 | — | — | — |
| 64 | 4 | 179.25 | 980.48 | 4 | 146.50 | 2121.52 |
| 128 | 4 | 346.75 | 455.69 | 4 | 330.00 | 844.62 |
| 256 | 4 | 533.25 | 280.96 | 4 | 520.75 | 541.97 |
| 512 | 4 | 917.50 | 282.07 | 4 | 861.00 | 361.08 |

this figure will be printed in b/w

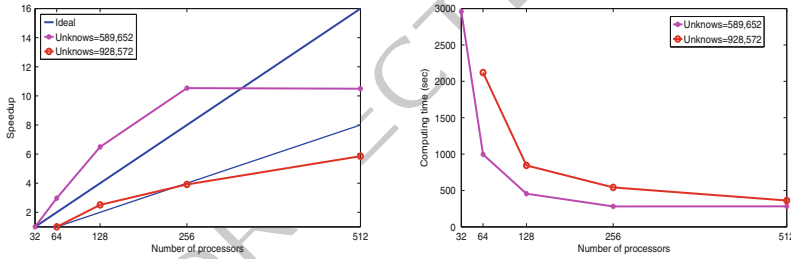


Fig. 6. The speedup and the total compute time for two different mesh sizes. $Re = 100$

as we increase the Re . On the other hand, we achieve higher percentage of reduction 152 of energy dissipation in the harder to solve situations.

Table 3. The impact of Re . $\beta = 0.1$, $overlap = 8$, $DOF = 589,652$, $np = 128$.

| Re | Newton | GMRES | Time | Energy Dissipation | | |
|------|--------|--------|---------|--------------------|-------|-----------|
| | | | | Init. | Opt. | Reduction |
| 100 | 4 | 346.75 | 456.83 | 1.17 | 1.13 | 3.42% |
| 200 | 4 | 372.00 | 470.16 | 0.65 | 0.62 | 4.62% |
| 300 | 6 | 671.00 | 871.19 | 12.56 | 11.80 | 6.05% |
| 600 | 7 | 721.71 | 1035.84 | 7.43 | 6.97 | 6.19% |

5 Conclusions and Future Work

154

We developed a parallel one-shot LNKSz for two-dimensional shape optimization problems governed by incompressible Navier-Stokes equations. We tested the algorithms for an artery bypass design problem with more than 900,000 DOF and up to 512 processors. The numerical results show that our method is quite robust with respect to the Re and the regularization parameter. The strong scalability is almost ideal when np is not too large. In the future, we plan to study some multilevel Schwarz methods which may improve the scalability when np is large.

Bibliography

162

- [1] F. Abraham, M. Behr, and M. Heinkenschloss. Shape optimization in stationary blood flow: A numerical study of non-Newtonian effects. *Comput. Methods Biomech. Biomed. Engng.*, 8:127–137, 2005.
- [2] V. Agoshkov, A. Quarteroni, and G. Rozza. A mathematical approach in the design of arterial bypass using unsteady Stokes equations. *J. Sci. Comput.*, 28:139–165, 2006.
- [3] S. Balay, K. Buschelman, V. Eijkhout, W. D. Gropp, D. Kaushik, M. G. Knepley, L. C. McInnes, B. F. Smith, and H. Zhang. PETSc Users Manual. Technical report, Argonne National Laboratory, 2010.
- [4] G. Biros and O. Ghattas. Parallel Lagrange-Newton-Krylov-Schur methods for PDE-constrained optimization. Part I: The Krylov-Schur solver. *SIAM J. Sci. Comput.*, 27:687–713, 2005.
- [5] O. Ghattas and C. Orozco. A parallel reduced Hessian SQP method for shape optimization. In N. M. Alexandrov and M.Y. Hussaini, editors, *Multidisciplinary Design Optimization: State of the Art*, pages 133–152. SIAM, Philadelphia, 1997.
- [6] M. D. Gunzburger. *Perspectives in Flow Control and Optimization: Advances in Design and Control*. SIAM, Philadelphia, 2003.
- [7] B. Mohammadi and O. Pironneau. *Applied Shape Optimization for Fluids*. Oxford University Press, Oxford, 2001.
- [8] E. Prudencio and X.-C. Cai. Parallel multilevel restricted Schwarz preconditioners with pollution removing for PDE-constrained optimization. *SIAM J. Sci. Comput.*, 29:964–985, 2007.
- [9] E. Prudencio, R. Byrd, and X.-C. Cai. Parallel full space SQP Lagrange-Newton-Krylov-Schwarz algorithms for PDE-constrained optimization problems. *SIAM J. Sci. Comput.*, 27:1305–1328, 2006.
- [10] A. Quarteroni and G. Rozza. Optimal control and shape optimization of aortic-coronary bypass anastomoses. *Math. Models and Methods in Appl. Sci.*, 13:1801–1823, 2003.
- [11] A. Toselli and O. Widlund. *Domain Decomposition Methods: Algorithms and Theory*. Springer-Verlag, Berlin, 2005.